

Relation-Guided Representation Learning

Zhao Kang^{a,b,*}, Xiao Lu^{a,*}, Jian Liang^c, Kun Bai^c, Zenglin Xu^{d,e,**}

^a*School of Computer Science and Engineering, University of Electronic Science and Technology of China, Sichuan, China*

^b*Trusted Cloud Computing and Big Data Key Laboratory of Sichuan Province*

^c*Cloud and Smart Industries Group, Tencent, Beijing, China*

^d*School of Computer Science and Technology, Harbin Institute of Technology, Shenzhen, China*

^e*Center for Artificial Intelligence, Peng Cheng Lab, Shenzhen, China*

Abstract

Deep auto-encoders (DAEs) have achieved great success in learning data representations via the powerful representability of neural networks. But most DAEs only focus on the most dominant structures which are able to reconstruct the data from a latent space and neglect rich latent structural information. In this work, we propose a new representation learning method that explicitly models and leverages sample relations, which in turn is used as supervision to guide the representation learning. Different from previous work, our framework well preserves the relations between samples. Since the prediction of pairwise relations themselves is a fundamental problem, our model adaptively learns them from data. This provides much flexibility to encode real data manifold. The important role of relation and representation learning is evaluated on the clustering task. Extensive experiments on benchmark data sets demonstrate the superiority of our approach. By seeking to embed samples into subspace, we further show that our method can address the large-scale and out-of-sample problem. Our source code is publicly available at: <https://github.com/nbShawnLu/RGRL>.

Keywords: deep auto-encoder, unsupervised representation learning, subspace clustering, pairwise relation

*These authors contributed equally

**Corresponding author

1. Introduction

Acquiring useful representations is crucial to the performance of numerous techniques in a wide range of fields, such as machine learning, computer vision, pattern recognition. Handcrafted representation based on some professional knowledge was widely used previously [1, 2, 3]. However, they are always limited to specific tasks or simple scenarios. Facing complex circumstances, they could severely degenerate. Therefore, learning task-friendly representations with little or no supervision has been a long-lasting yet challenging topic in artificial intelligence [4, 5, 6, 7, 8, 9].

During the last decade, deep auto-encoders (DAEs) have achieved great success in unsupervised representation learning and considerable gains are obtained consequently [10, 11, 12, 13, 14, 15]. Basically, the goal of auto-encoders is to learn a mapping of the input data to a lower-dimensional representation space which succinctly captures the statistics of an underlying data distribution [16]. Most methods simply combine a well-designed clustering assignment loss with reconstruct loss [17, 18, 19, 20]. Some methods take pairwise relations and graphs into consideration [21, 22]. Recently, adversarial strategy has been widely used with DAEs to improve representation and clustering robustness [23, 24, 25]. In multi-view clustering, shared generative latent representation learning [26] learns a shared latent representation under the VAE framework. AE²-Nets [27] jointly learns the representation of each view and encodes them into an intact latent representation with a nested auto-encoder framework. Affine Equivariant Autoencoder (AEAE) [28] learns features that are equivariant to the affine transformation.

Though impressive performance has been achieved, some important structural information, e.g., pairwise relation, is not well taken care of [29]. Pairwise relations, i.e., similarities, between data samples play an important role in many applications of artificial intelligence [30, 31, 32, 33]. Many traditional dimensionality reduction methods such as kernel PCA [34, 35], isomap [36], t-SNE [37], matrix factorization [7], and locally linear embedding (LLE) [36] find low-dimensional representations of data samples by feat of retaining their pairwise relations or local neighborhoods in the embedding space.

Besides implicit usage in dimensionality reduction task, pairwise relation is also a fundamental quantity in many other applications, e.g., k -nearest neighbor search, classification [38], clustering [7, 39, 40, 41, 42], kernel methods [43, 32, 44]. In particular, the performance of spectral clustering [45, 46] heavily depends on the quality of the input similarity graph matrix. The

prediction of pairwise relations themselves is at the heart of these methods [47, 48]. Pre-defined pairwise relation is rather heuristic and might not be able to reflect the intrinsic data structure. It will be highly desirable to be able to automatically learn pairwise relation that would work the underlying data [49].

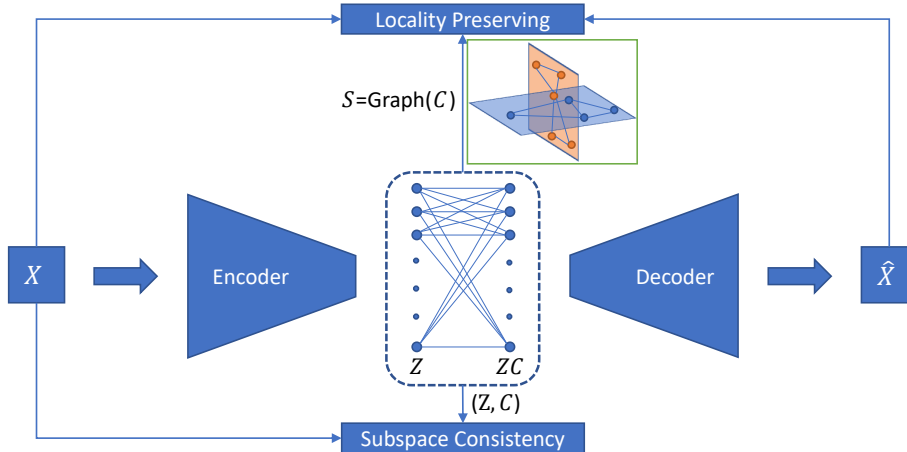


Figure 1: Architecture of RGRL. The input X is mapped to Z through an encoder, Z is self-expressed by ZC , and then reconstructed as \hat{X} through a decoder. Pairwise relation C guides the learning process of low-dimensional representation. Instead of self-reconstruction in conventional auto-encoder, weighted reconstruction is applied to preserve locality structure information. Subspace consistency is harnessed to ensure the cluster structure is not hurt after the transformation.

In this paper, we explore a data-driven approach to learn pairwise relation and low-dimensional representation simultaneously, named Relation-Guided Representation Learning (RGRL). RGRL takes advantage of relations among samples. Specifically, to discover the underlying manifold structure and obtain a more informative representation, we don't adopt the widely used reconstruction loss in auto-encoder, i.e., each instance is reconstructed by itself, which fails to explicitly model the data relation. In our framework, each instance x_i is reconstructed by a set of instances \hat{x}_j weighted by the corresponding relation between them, so as to satisfy locality preserving. Rather than using fixed relations, we iteratively learn them from data. This learning process is based on the self-expression property, i.e., each sample can be represented by a linear combination of other samples in the same subspace. Moreover, this relation should hold for both raw data and embeddings, i.e.,

subspace consistency.

The framework of our method is displayed in Figure 1. The weights of the self-expression layer correspond to the combination coefficient C , i.e., the relations between data instances. Locality preserving ensures the reconstruction of data, while subspace consistency guarantees pairwise relations hold before and after transformation. Although the fundamental idea applies to data in many tasks, we focus on clustering in this paper.

In summary, our contributions can be summarized as:

- We explicitly model and leverage relations between samples to guide the representation learning for deep auto-encoder. The embedded representations well preserve the local neighborhood structure on the data manifold.
- The proposed method learns pairwise relation or similarity and maintains its consistency in both input space and embedding space. Consequently, the subspace or cluster structure is retained.
- Extensive experiments on clustering, similarity learning, and embedding demonstrate the superiority of our method. In particular, we show how to tackle large-scale data challenge based on out-of-sample approach.

The paper is organized as follows: Section 2 gives a brief review about related works. Section 3 introduces locality preserving and subspace consistency, then we propose our relation-guided representation learning method. In Section 4, we implement our method on clustering task and compare with some related methods. In Section 5, we extend our method for large-scale datasets and examine embedding performance with experiments. The paper is concluded in Section 6.

2. Related Work

In this paper, we concentrate on relation preserving embedding construction, similarity learning, and its application to clustering. Thus, we give a brief review of some related work.

Deep auto-encoder aims to compress data $X \in \mathcal{R}^{d \times n}$ into low-dimensional representation $Z \in \mathcal{R}^{k \times n}$ where $k \ll d$, which in turn reconstructs the original data. It is often composed of an encoder F and a decoder G with mirror construction. Their parameters are denoted as Θ_e and Θ_d , respectively.

Specifically, an auto-encoder can be optimized by objective function

$$\min_{\Theta_e, \Theta_d} \sum_{i=1}^n \|X_i - G_{\Theta_d}(F_{\Theta_e}(X_i))\|^2. \quad (1)$$

Though this basic model has led to far-reaching success for data representation, it forces to reconstruct its input without considering other data points present in the data [29]. To overcome this limitation, [50] proposes a generalized auto-encoder framework to capture the local manifold structure. The relation is pre-calculated based on some heuristic functions, e.g., Cosine, Gaussian. This approach has one inherent limitation, i.e., it might not be appropriate to the structure of the data space [51]. In deep manifold clustering (DMC) [52], the authors interpret the locality of manifold as similar inputs should have similar representations, and minimize the reconstruction of X_i itself and its local neighborhood. However, they define reconstruction weights either in a supervised or pre-defined way and the relations between samples are not flexible for modeling.

To keep locality properties on latent space is another way to get effective representations. The deep embedding network (DEN) [53] first learns representations from an auto-encoder while keeps locality-preserving and group sparsity constraints on low-dimension space. It requires that two latent representations should be similar if they are similar in the original space defined by Gaussian kernel. The deep embedded clustering (DEC) [17] method fine-tunes the encoder by minimizing KL divergence between soft assignment and target distribution. The improved deep embedded clustering (IDEC) [18] improves DEC by remaining decoder in fine-tune stage. The recently developed deep k -means (DKM) [54] jointly learns latent representations and k -means.

Motivated by the success of subspace clustering method, deep subspace clustering (DSC) [22] implements subspace clustering method in deep neural network and achieves promising results. However, DSC only assumes the subspace structure in latent space, which fails to make full use of the original data, and forces to reconstruct all parts of the input, even if they are contaminated by noise or outliers. [55] points out that different layers of the encoder provide different information and it is difficult to find a suitable subspace clustering representation by only relying on the output of the encoder. This provides us a strong motivation to incorporate original information to enhance the clustering performance. The deep adversarial subspace clustering (DASC) [24] improves DSC by introducing adversarial learning so that

Table 1: Comparison of recently proposed unsupervised learning methods with our approach. CNN denotes using convolutional neural network, SL denotes subspace learning, LP denotes the locality preserving, SC denotes subspace consistency.

Approach	DMC	DEC	IDEC	DKM	DSC	DEPICT	DSCDAN	RGRL
CNN	✗	✗	✗	✗	✓	✗	✗	✓
SL	✗	✗	✗	✗	✓	✗	✗	✓
LP	✓	✗	✓	✗	✗	✓	✓	✓
SC	✗	✗	✗	✗	✗	✗	✗	✓

the discriminator can evaluate the clustering quality and supervise the generator’s learning. [56] addresses the outliers and initialization issues by adding a weighted subspace network.

Recently, self-supervised learning becomes a popular tool of unsupervised learning which uses pretext tasks to replace the labels annotated by humans[57, 58]. The DeepCluster [11] uses the cluster assignments as pseudo-labels to learn the parameters of the network. The deep comprehensive correlation mining (DCCM) [59] makes use of the local robustness assumption and utilizes above pseudo-graph and pseudo-label to learn better representation. The self-supervised convolutional subspace clustering (S²ConvSCN) [60] introduces a spectral clustering module and a classification module into DSC, i.e., applying the current clustering results to supervise the training of network. All deep subspace clustering methods have large cost of memory due to the self-expression layer structure, which hinders their applications on large-scale data sets. This explains why all DSC methods use small datasets.

In this paper, we aim to learn representations guided by locality preserving and global subspace consistency using a simple and neat model. We compare our method with some of the related work in Table 1. We can clearly see the advantage of our approach. Meanwhile, more complicated modules and tricks can be easily apply on the top of our fundamental model.

3. The Proposed Method

We propose a deep auto-encoder network to learn representations of the data guided by the relation between samples. The proposed approach is composed of four key components: 1) the encoder F encodes X into latent representation Z , 2) the decoder G reconstructs \hat{X} from latent representation, 3) the locality preserving module, 4) the subspace consistency module. Our goal is to train a reconstruction such that \hat{X}_i is not only similar to X_i , but also to other samples X_j determined by their relations C_{ij} . Notably, our used

network architecture is similar to DSC [22]. Different from DSC, our main contribution lies in the design of two different objective terms, i.e., locality preserving and subspace consistency, aiming to fully exploit the relations among data points. By contrast, DSC applies traditional self-reconstruction loss and self-expression only in latent space.

3.1. Locality Preserving

To preserve the local structure, we use the weighted reconstruction instead of Eq.(1). To be precise, X_i is reconstructed by \hat{X}_j with weight S_{ij} , where S_{ij} is the similarity between samples X_i and X_j . Samples with large distance should have low similarity. Then, the network can be trained by solving

$$\min_{\Theta_e, \Theta_d} \sum_{ij} S_{ij} \|X_i - G_{\Theta_d}(F_{\Theta_e}(X_j))\|^2. \quad (2)$$

Compared to self-reconstruction, Eq.(2) can characterize the neighborhood relations of samples. In other words, the learned latent representation learned is encoded by neighborhood relations. Eq.(2) can be further transformed as follows

$$\begin{aligned} \sum S_{ij} \|X_i - \hat{X}_j\|^2 &= \sum S_{ij} (\|X_i\|^2 - 2X_i^T \hat{X}_j + \|\hat{X}_j\|^2) \\ &= \sum S_{ij} [(\|X_i\|^2 - 2X_i^T \hat{X}_i + \|\hat{X}_i\|^2) \\ &\quad + 2(X_i^T \hat{X}_i - X_i^T \hat{X}_j)] \\ &= Tr[(X - \hat{X})^T D(X - \hat{X})] \\ &\quad + 2Tr(X^T L \hat{X}), \end{aligned} \quad (3)$$

where diagonal matrix $D = Diag(\sum_{j=1}^n S_{ij})$ and $L = D - S$ is the Laplacian matrix. We can see that similarity matrix S would be crucial to the performance of the network. Unlike many existing work using pre-defined values, we propose to automatically learn S from data.

3.2. Subspace Consistency

Recently, similarity learning based on self-expression has been widely used. Its basic idea is that each sample can be represented by a linear combination of other samples in the same subspace [61, 62, 63]. This combination

coefficient represents the relation between samples. In general, it solves the following problem

$$\min_C \frac{1}{2} \|X - XC\|_F^2 + \alpha \|C\|_p \quad s.t. \quad \text{diag}(C) = 0, \quad (4)$$

where the first term minimizes the reconstruction error, the second term is certain regularizer function on C , and α is a balance parameter. Matrix C can represent the subspace structure of data, i.e., $C_{ij} = 0$ if the i -th sample and j -th sample do not lie in the same subspace.

In our case, we have two representations, i.e., original space X and latent space Z_{Θ_e} . We expect the subspace structure can be well preserved after the transformation, i.e., subspace consistency. Therefore, we also minimize the self-expression error in latent space. DSC [22] fails to consider the subspace structure in the raw space. Then, our objection function becomes

$$\min_C \frac{1}{2} \|X - XC\|_F^2 + \frac{\beta}{2} \|Z_{\Theta_e} - Z_{\Theta_e}C\|_F^2 + \alpha \|C\|_p \quad (5)$$

$$s.t. \quad \text{diag}(C) = 0.$$

In the network, we add a fully connected layer without bias between the encoder and the decoder, whose weights represent the coefficient matrix C , so-called the self-expression layer as shown in Fig 1 [22]. By solving Eq.(5), we can obtain the sample relation matrix C . Then, the similarity is usually computed based on $S = \frac{1}{2}(|C| + |C|^T)$. Since the scale of each row and column of similarity matrix might be different, we use the symmetric normalized Laplacian for scale normalization while keeping the symmetry of the similarity matrix S [46]. Specifically, normalized degree matrix $D_n = I$ and normalized Laplacian matrix $L_n = D^{-\frac{1}{2}}LD^{-\frac{1}{2}}$. Then, we have $Tr[(X - \hat{X})^T D_n (X - \hat{X})] = \|X - \hat{X}\|_F^2$.

3.3. Proposed Formulation

To jointly train the network with relation guided by both subspace consistency and locality preserving, we combine above terms together, which yields

$$L(\Theta) = \|X - \hat{X}_\Theta\|_F^2 + 2Tr(X^T L_n \hat{X}_\Theta) + \alpha \|C\|_p$$

$$+ \frac{\beta}{2} \|Z_{\Theta_e} - Z_{\Theta_e}C\|_F^2 + \frac{\gamma}{2} \|X - XC\|_F^2 \quad (6)$$

$$s.t. \quad \text{diag}(C) = 0,$$

Table 2: Statistics of the datasets.

Dataset	EYaleB	ORL	MNIST	Umist	COIL20	COIL40
Samples	2,432	400	1,000	480	1,440	2,880
Classes	38	40	10	20	20	40
Dimensions	48×42	32×32	28×28	32×32	32×32	32×32

where Θ denotes the network parameters, which include encoder parameters Θ_e , self-expression layer parameters C , and decoder parameters Θ_d . Note that, the output \hat{X} of the decoder is a function of $\{\Theta_e, C, \Theta_d\}$. In fact, all the unknowns in Eq.(6) are functions of network parameters. This network can be implemented by neural network frameworks and trained by back-propagation. Once the network architecture is optimized, we obtain the lower-dimensional representation Z and relation matrix C .

Compared to the existing work in the literature, our proposed RGRL has the following advantages:

- The proposed model takes into account the data relation, which outputs relation preserving representations.
- The designed architecture also performs similarity learning. This solves another fundamental problem. Moreover, we convert the similarity learning into network parameters optimization problem .

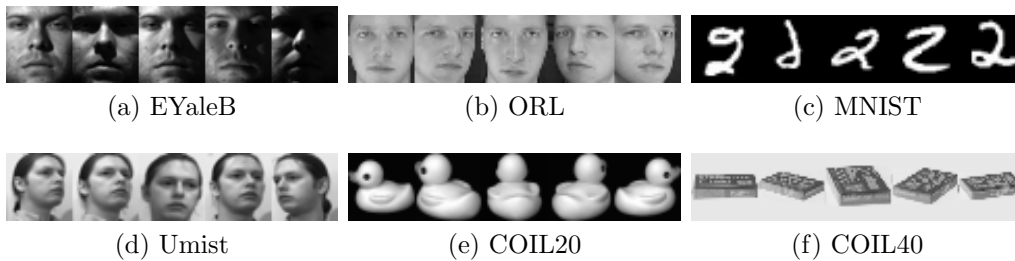


Figure 2: Examples of the datasets.

4. Similarity Learning Experiments

In this section, we evaluate the similarity learning effect on the clustering task.

Table 3: Network settings for clustering experiments, including the “kernel size@channels” and size of C .

	EYaleB	ORL	MNIST	Umist	COIL20	COIL40
encoder	5×5@10	5×5@5	5×5@15	5×5@20	3×3@15	3×3@20
	3×3@20	3×3@3	3×3@10	3×3@10	-	-
	3×3@30	3×3@3	3×3@5	3×3@5	-	-
C	2432×2432	400×400	1000×1000	480×480	1440×1440	2880×2880
decoder	3×3@30	3×3@3	3×3@5	3×3@5	3×3@15	3×3@20
	3×3@20	3×3@3	3×3@10	3×3@10	-	-
	5×5@10	5×5@5	5×5@15	5×5@20	-	-

4.1. Datasets

We perform experiments on three widely used face datasets: ORL, Extended Yale B (EYaleB), Umist; and three object datasets: MNIST, COIL20, and COIL40. ORL is composed of 40 subjects, each subject has 10 images taken with varying poses and expressions. EYaleB contains 38 subjects each with 64 images taken under different illumination. Umist only contains 20 individuals, each person has 24 images taken under very different poses. COIL20 has 20 classes of toys with 72 images in each class. COIL40 has 40 classes of objects with 72 images in each class. For MNIST, we use the first 100 images of each digit. The statistics of the datasets are summarized in Table 2. Some examples of the datasets are shown in Fig 2.

4.2. Experimental Setup

In this experiment, we use convolutional neural networks with ReLU activation function to implement the encoder and decoder. We use one layer convolutional network for COIL20 and COIL40, and three layers convolutional network for others. The architecture details of the networks are shown in Table 3.

We first pre-train the encoder and decoder without the self-expression layer. Then we fine-tune the whole network. We fix regularization parameter α as 1e-4 and perform grid searching for β and γ . We use Adam [64] as the optimizer. Learning rate is set as 1e-3 in pre-training, and 1e-4 in fine-tune stage. Our method is implemented with Tensorflow and the experiments are run on a server with an NVIDIA TITAN Xp GPU, 12GB GRAM.

We implement a spectral clustering algorithm after we obtain the weight C . Spectral clustering [46] is a popular clustering technique with promising

performance. Nevertheless, it is always challenging to construct an appropriate similarity graph that is most suitable for the specific dataset at hand. To examine the performance of learned coefficient matrix C , we use the coefficient matrix to build an affinity matrix A , as input to the spectral clustering algorithm. To enhance the block-structure and improve the clustering accuracy, we employ the approach proposed in efficient dense subspace clustering (EDSC) [65], which can be summarized as Algorithm 1, where α is empirically selected according to the level of noise and d is the maximal intrinsic dimension of subspaces. For fairness, we use the same setting as deep subspace clustering network (DSC) [22].

Algorithm 1 Compute affinity matrix.

Input: The relation matrix, C ;

The number of cluster, k ;

The intrinsic dimension of subspaces, d ;

Output: The affinity matrix, A ;

- 1: Let $S = \frac{1}{2}(|C| + |C|^T)$;
 - 2: Compute the SVD of S , $S = U\Sigma V^T$;
 - 3: Let $Z = U_m \Sigma_m^{\frac{1}{2}}$, where $m = k * d + 1$;
 - 4: Compute affinity matrix $A = [ZZ^T]^\alpha$;
-

We compare with closely related shallow and deep techniques developed in recent years. They include: low rank representation (LRR) [66], low rank subspace clustering (LRSC) [67], sparse subspace clustering (SSC) [61], kernel sparse subspace clustering (KSSC) [68], SSC by orthogonal matching pursuit (SSC-OMP) [69], efficient dense subspace clustering (EDSC) [65], SSC with pre-trained convolutional auto-encoder features (AE+SSC), deep subspace clustering network with ℓ_1 -norm (DSC-L1) [22], deep subspace clustering network with ℓ_2 -norm (DSC-L2), deep embedding clustering (DEC) [17], deep k -means (DKM) [54], deep comprehensive correlation mining (DCCM) [59], deep embedded regularized clustering (DEPICT) [13], and deep spectral clustering using dual autoencoder network (DSCDAN) [70].

Three widely used evaluation metrics are used to evaluate the performances: accuracy (ACC), normalized mutual information (NMI), and purity (PUR) [71, 72].

Table 4: Clustering results of RGRL and compared methods on MNIST, EYaleB, ORL, COIL20, COIL40, and Umist. For the sake of space, we only list results of RGRL_{sc} with ℓ_2 -norm.

Dataset	Metric	SSC	ENSC	KSSC	SSC-OMP	EDSC	LRR	LRSC	AE+SSC	DSC-L1	DSC-L2	DEC	DKM	DCCM	DEPICT	DSCDAN	RGRL _{sc} -L2	RGRL-L1	RGRL-L2
MNIST	ACC	0.4530	0.4983	0.5220	0.3400	0.5650	0.5386	0.5140	0.4840	0.7280	0.7500	0.6120	0.5332	0.4020	0.4240	0.7450	0.7570	0.8130	0.8140
	NMI	0.4709	0.5495	0.5623	0.3272	0.5752	0.5632	0.5576	0.5337	0.7217	0.7319	0.5743	0.5002	0.3468	0.4236	0.7110	0.7323	0.7534	0.7552
	PUR	0.4940	0.5483	0.5810	0.3560	0.6120	0.5684	0.5550	0.5290	0.7890	0.7991	0.6320	0.5647	0.4370	0.3560	0.7480	0.7980	0.8150	0.8160
EYaleB	ACC	0.7354	0.7537	0.6921	0.7372	0.8814	0.8499	0.7931	0.7480	0.9681	0.9733	0.2303	0.1713	0.1176	0.1094	0.7307	0.9840	0.9757	0.9753
	NMI	0.7796	0.7915	0.7359	0.7803	0.8835	0.8636	0.8264	0.7833	0.9687	0.9703	0.4258	0.2704	0.2011	0.1594	0.8808	0.9776	0.9668	0.9661
	PUR	0.7467	0.7654	0.7183	0.7542	0.8800	0.8623	0.8013	0.7597	0.9711	0.9731	0.2373	0.1738	0.1312	0.1044	0.7644	0.9840	0.9757	0.9753
ORL	ACC	0.7425	0.7525	0.7143	0.7100	0.7038	0.8100	0.7200	0.7563	0.8550	0.8600	0.5175	0.4682	0.6250	0.2800	0.7950	0.8700	0.8650	0.8700
	NMI	0.8459	0.8540	0.8070	0.7952	0.7799	0.8603	0.8156	0.8555	0.9023	0.9034	0.7449	0.7332	0.7906	0.5764	0.9135	0.9189	0.9169	0.9215
	PUR	0.7875	0.7950	0.7513	0.7463	0.7138	0.8225	0.7542	0.7950	0.8585	0.8625	0.5400	0.4752	0.5975	0.1450	0.8025	0.8775	0.8775	0.8850
COIL20	ACC	0.8631	0.8760	0.7087	0.6410	0.8371	0.8118	0.7416	0.8711	0.9314	0.9368	0.7215	0.6651	0.8021	0.8618	0.7868	0.9451	0.9694	0.9701
	NMI	0.8892	0.8952	0.8243	0.7412	0.8828	0.8747	0.8452	0.8900	0.9353	0.9408	0.8007	0.7971	0.8639	0.9266	0.9131	0.9607	0.9748	0.9762
	PUR	0.8747	0.8892	0.7497	0.6667	0.8585	0.8361	0.7937	0.8901	0.9306	0.9397	0.6931	0.6964	0.7889	0.8319	0.7819	0.9451	0.9694	0.9701
COIL40	ACC	0.7191	0.7426	0.6549	0.4431	0.6870	0.6493	0.6327	0.7391	0.8003	0.8075	0.4872	0.5812	0.7691	0.8073	0.7385	0.8135	0.8292	0.8396
	NMI	0.8212	0.8380	0.7888	0.6545	0.8139	0.7828	0.7737	0.8318	0.8852	0.8941	0.7417	0.7840	0.8890	0.9291	0.8940	0.9194	0.9246	0.9284
	PUR	0.7716	0.7924	0.7284	0.5250	0.7469	0.7109	0.6981	0.7840	0.8646	0.8740	0.4163	0.6367	0.7663	0.8191	0.7726	0.8497	0.8594	0.8594
Umist	ACC	0.6904	0.6931	0.6531	0.6438	0.6937	0.6979	0.6729	0.7042	0.7242	0.7312	0.5521	0.5106	0.5458	0.4521	0.6937	0.7458	0.8104	0.8104
	NMI	0.7489	0.7569	0.7377	0.7068	0.7522	0.7630	0.7498	0.7515	0.7556	0.7662	0.7125	0.7249	0.7440	0.6329	0.8816	0.8612	0.8812	0.8812
	PUR	0.6554	0.6628	0.6256	0.6171	0.6683	0.6670	0.6562	0.6785	0.7204	0.7276	0.5917	0.5685	0.5854	0.4167	0.7167	0.7875	0.8354	0.8354

Accuracy is defined as:

$$\text{ACC} = \frac{\sum_{i=1}^N \delta(\text{map}(l_i) = y_i)}{N}, \quad (7)$$

where δ is an indicator function, l_i is the clustering label for X_i produced by spectral clustering, map transforms the clustering label l_i to its group label based on Kuhn-Munkres algorithm, and y_i is the ground truth label of X_i .

Normalized mutual information is another popular metric used for evaluating clustering tasks. It is defined as follows:

$$\text{NMI}(Y, L) = \frac{I(Y, L)}{\sqrt{H(Y)H(L)}}, \quad (8)$$

where Y and L respectively denote ground truth label and clustering label. I is mutual information which measures the information gain to the true partition after knowing the clustering result, H is entropy and $\sqrt{H(Y)H(L)}$ is used to normalize the mutual information.

Purity is a simple and transparent evaluation measure which is defined as:

$$\text{PUR}(Y, L) = \frac{\sum_{i=1}^k \max_j |L_i \cap Y_j|}{N}, \quad (9)$$

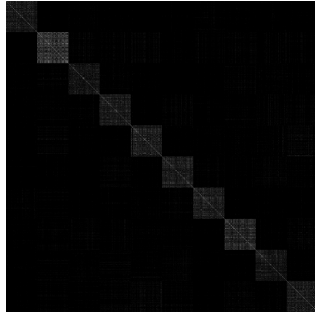
where Y is the set of classes and L is the set of clusters, k is the number of clusters, L_i denotes the set of samples belongs to i -th cluster, Y_j denotes the set of samples belongs to j -th class.

To examine the strength of locality preserving by using weighted reconstruction, we made an ablation study by replacing the weighted reconstruction with original auto-encoder reconstruction, dubbed RGRL_{sc} , since it only has the subspace consistency effect.

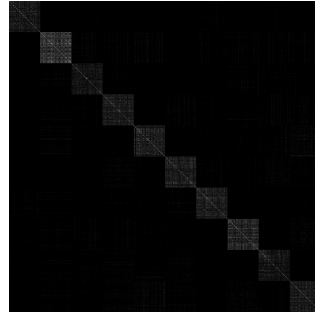
4.3. Results

Clustering results based on similarity learning is recorded in Table 4. As observed, our method achieves the best performance among these related methods in most cases. Besides, we have these observations:

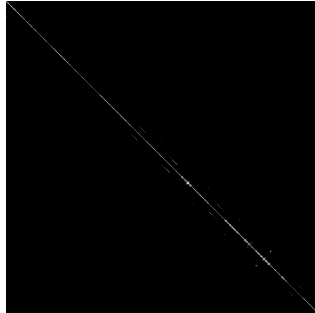
- RGRL outperforms shallow subspace clustering methods significantly. This mainly attributes to the powerful representation ability of neural networks.
- RGRL significantly improves performance compared to other deep clustering methods. It benefits from the supervision of sample relations.
- RGRL performs better than RGRL_{sc} on all datasets except EYaleB. For example, in terms of accuracy, RGRL outperforms RGRL_{sc} by about 6% on MNIST and Umist. This verifies the importance of locality preserving.
- With respect to deep subspace clustering, the improvement is also impressive. For instance, accuracy improves by 8% on Umist. Moreover, DASC [24] and $\text{S}^2\text{ConvSCN}$ [60] are also two related methods. Since they have not released their code, we directly cite their results on the datasets we both used. On COIL20/COIL40, our acc is 0.9701/0.8396, while DASC gives 0.9639/0.8354. On MNIST, our acc is 0.8140, while DASC gives 0.8040. On Umist, our acc is 0.8104, while DASC gives 0.7688. On EYaleB, ours is 0.984, while DASC gives 0.9856, $\text{S}^2\text{ConvSCN}$ gives 0.9848. On ORL, ours is 0.87, while DASC gives 0.8825, $\text{S}^2\text{ConvSCN}$ gives 0.895. It proves that our proposed method is comparable or even better in some cases w.r.t. them. Note that, they come with some complicated components, such as adversarial learning and label supervision. By contrast, our proposed framework is very simple and can also incorporate those modules to further enhance the performance.
- DEC, DKM, and DCCM perform even worse than shallow approaches. This is due to the fact that they use Euclidean distance or cosine distance to evaluate pairwise relation, which fails to capture the complex



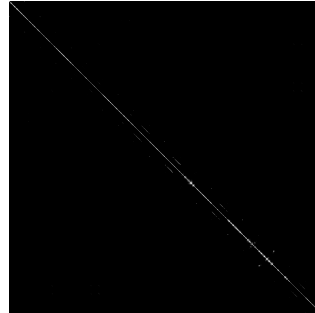
(a) MNIST-L1



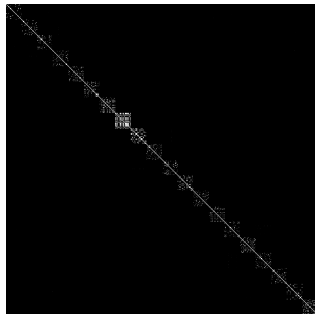
(b) MNIST-L2



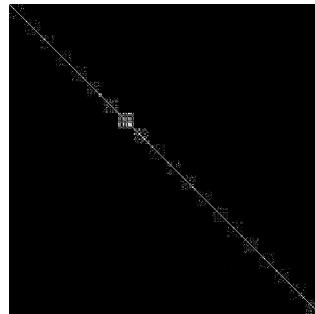
(c) COIL20-L1



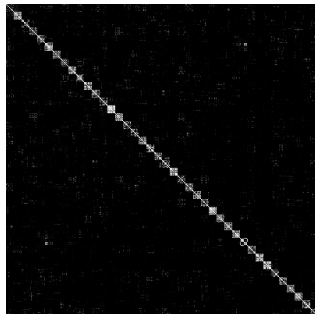
(d) COIL20-L2



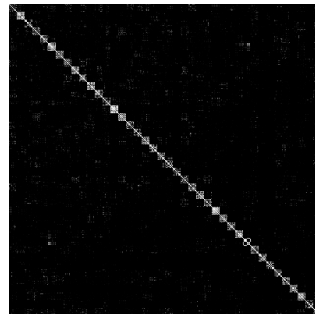
(e) Umist-L1



(f) Umist-L2



(g) ORL-L1



(h) ORL-L2

Figure 3: Visualization of learned affinity matrix A on the datasets.

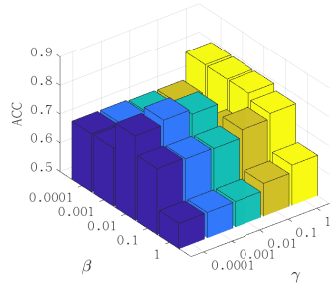
manifold structure. In general, subspace learning approach works much better in this situation. Compared to our method, DEPICT [13] and DSCDAN [70] produce inferior performance. With respect to DEPICT, the performance of DSCDAN is more stable.

To intuitively show the merit of our similarity learning approach, we visualize the affinity matrix A in Fig. 3, where A_{ij} indicates the similarity between X_i and X_j and brighter pixel means higher similarity. Since the indexes of samples are sorted by classes, the ideal matrix should have a block-diagonal structure. It can be seen that the similarity matrix A learned by our algorithm well exhibits this block-diagonal property and it is hard to detect much difference between ℓ_1 and ℓ_2 -norm. In particular, for the MNIST data set, the block size is relatively large since each cluster contains the most points. It can be observed that the block is very obvious, which indicates that the energy is more evenly distributed within each class. For the Umist dataset, it contains 20 classes and each single block only consists of 24 samples. The ORL data set contains 40 classes and each block only contains 10 instances. Therefore, it is a very challenging data. By observing Fig. 3g and 3h, we can see that the energy distribution still satisfies the block-diagonal property and the similarity within each class is relatively uniform, which guarantees a good performance.

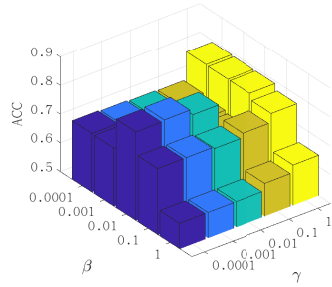
It is worth noting that Figs. 3c and 3d are quite different from others. More concretely, the energy of similarity graph is mainly distributed on the diagonal and its very small neighborhood, which means that each sample only has a strong connection with few nearby points. This phenomenon could possibly be explained by the acquisition process of COIL20. COIL20 has 20 kinds of objects and each picture is obtained by taking a photo every 5 degrees of rotation. As a result, each picture has a very strong connection to the photos with similar angles, especially the two that are taken before and after it. In addition, notice that some small dots reside on a line parallel to the diagonal line. They correspond to the first and the last sample in each class, which are supposed to be similar. The similarity between different classes is still small, so that each class can be finally separated.

4.4. Parameter Analysis

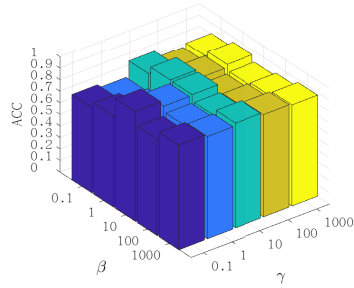
There are three hyper-parameters in our model: α , β and γ . As mentioned earlier, α is fixed as $1e-4$. We show the variation of accuracy along with the



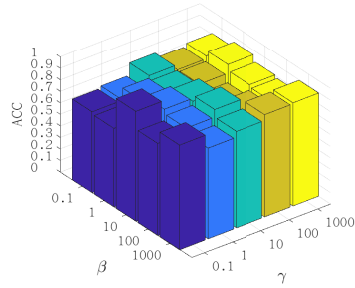
(a) MNIST-L1



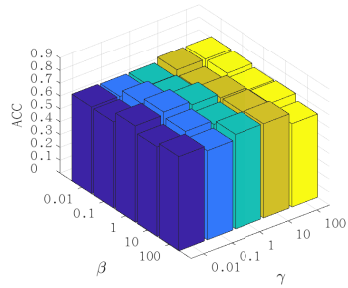
(b) MNIST-L2



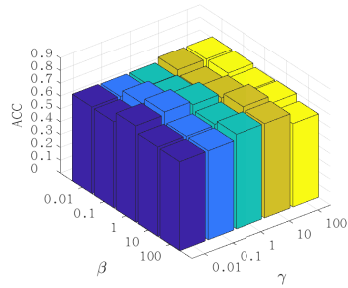
(c) COIL20-L1



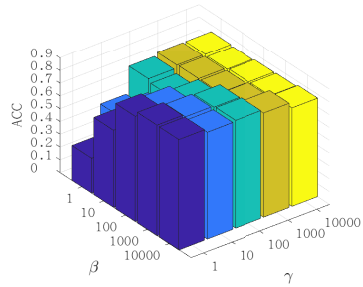
(d) COIL20-L2



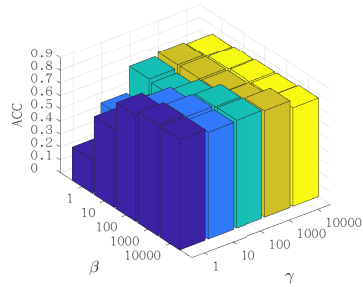
(e) Umist-L1



(f) Umist-L2



(g) ORL-L1



(h) ORL-L2

Figure 4: The influence of parameters on accuracy of the datasets.

Table 5: Statistics of the large datasets.

Dataset	MNIST	USPS	RCV1
Samples	70,000	9,298	10,000
Classes	10	10	4
Dimensions	28× 28	16× 16	2,000

change of β and γ in Fig. 4. Generally speaking, parameters are data-specific. Thus, different ranges are searched for different data sets. It can be seen that the performance on MNIST is very sensitive to the value of β , which means that subspace consistence plays a crucial role. For other datasets, our method works well for a wide range of values. One possible reason for the fluctuations is due to the fact that spectral clustering method is sensitive to the graph. It is well-known that a small disturbance in graph can lead to a large difference in clustering performance.

Table 6: Clustering results on MNIST, USPS, and RCV1.

Dataset	Metric	KM	AE+KM	DCN	IDEC	DKM	DCCM	DEPICT	DSCDAN	RGRL-L1	RGRL-L2
MNIST	ACC	0.535	0.808	0.811	0.857	0.840	0.655	0.9295	0.8189	0.9127	0.9127
	NMI	0.498	0.752	0.757	0.864	0.796	0.679	0.8799	0.8727	0.8175	0.8175
USPS	ACC	0.673	0.729	0.730	0.752	0.757	0.686	0.8565	0.8061	0.9148	0.9170
	NMI	0.614	0.717	0.719	0.749	0.776	0.675	0.8652	0.8507	0.8449	0.8320
RCV1	ACC	0.508	0.567	0.567	0.595	0.583	-	-	-	0.6852	0.6867
	NMI	0.313	0.315	0.316	0.347	0.331	-	-	-	0.4019	0.4030

5. Out-of-sample Experiments

In this section, we further show that our method can be extended to address large-scale and out-of-sample problem by embedding samples into subspace.

5.1. Datasets

The datasets used in this experiment are large clustering collections, each is composed of more than 9,000 samples. We perform experiments on two object datasets: MNIST and USPS; a text dataset: RCV1. We use full MNIST dataset which has 70,000 hand-written digits images in 10 classes. USPS contains 9,298 hand-written digits images in 10 classes. RCV1 contains around 810,000 English news stories labeled with a category tree. Following DKM [54], we randomly sample 10,000 documents from the four largest categories: corporate/industrial, government/social, markets and economics of RCV1,

each sample only belongs to one of these four categories. Note that, different from experiments in DEC [17] and IDEC [18], we keep samples with multiple labels only if they don't belong to any two of selected four categories. For text datasets, we select 2000 words with the highest tf-idf values to represent each document. The statistics of datasets in this experiment are summarized in Table 5.

5.2. Experimental Setup

Different from the above experiment, we use latent representations for clustering task. In particular, we train the network with a reasonable small batch of samples (5,000 samples for each dataset in our experiments), then we use the similarity matrix to predict the pseudo-labels of selected samples by the above approach. Finally, we encode all the data into latent space and use a nearest-neighbor classifier to predict the labels for the rest of the data. Following this approach, our method can address out-of-sample problem.

For fair of comparison, we use the same encoder/decoder architecture as DEC [17], IDEC [18], and DKM [54]. The encoder is a fully connected network with dimensions of d -500-500-2000- k for all datasets, where d is the dimension of input features and k is the number of clusters. And the decoder correspondingly is a mirror of the encoder, a fully connected network with dimensions of k -2000-500-500- d . A ReLU activate function is applied for each layer except the input, output, and embedding layer. We pre-train the auto-encoder 50 epochs and fine-tune the whole network with objective function (6) 30 epochs.

We compare our method with the k -means clustering (KM), an auto-encoder followed by k -means applied to the latent representation (AE+KM), and recent deep clustering approaches: deep clustering network (DCN) [19], IDEC [18], DKM [54], DCCM [59], DEPICT [13], and DSCDAN [70]. Since DCCM, DEPICT, and DSCDAN are designed for image dataset, they can not apply to text data RCV1.

5.3. Results

Clustering performance of embedding experiment is recorded in Table 6. Our method still outperforms recent deep clustering methods. In particular, compared to recent DKM, RGRL-L2 improves accuracy by 7.27%, 16%, and 10.37% on those three datasets, respectively. With regard to DCCM and DSCDAN, the accuracy improvement is more than 20% and 10%, respectively. The accuracy of our method is a little bit lower than DEPICT on

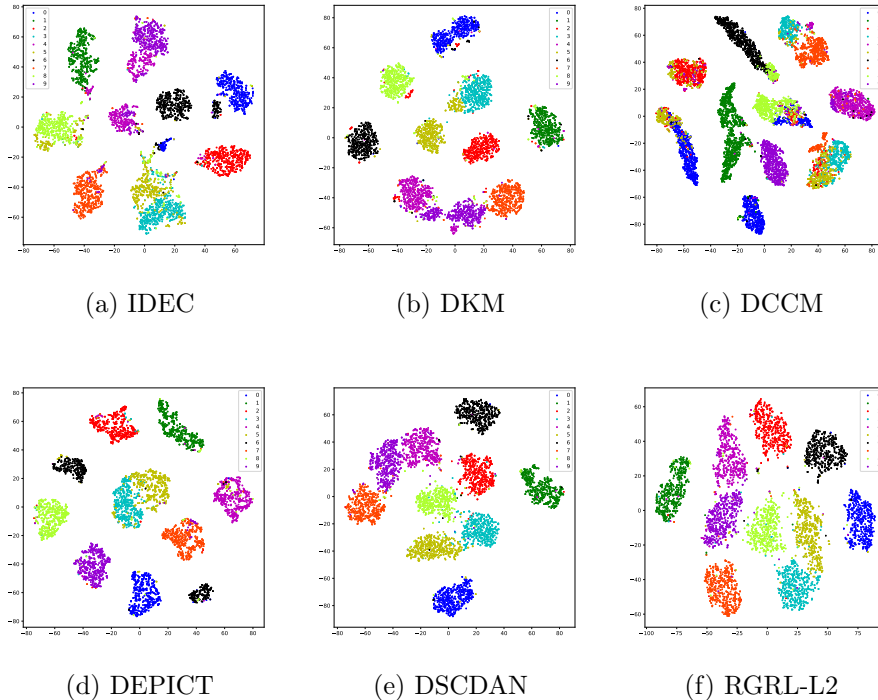


Figure 5: 2D visualization of the embedding spaces learned on USPS dataset.

MNIST, but it is improved by 6% on USPS. These benefits from embedding samples into subspaces. Therefore, our method proved to be an attractive technique to deal with large scale and out-of-sample problem.

We use the t-SNE method to visualize the learned latent representations of four most recent methods. As we can observe from Fig. 5, samples of different classes tangle in IDEC and DKM, which is because they force samples to move to cluster centers. Same phenomenon happens on DCCM since it is supervised by pseudo-graph guided by cosine similarity. For DEPICT, the black points are located in two separate places, which could degrade the performance. For DSCDAN, we can see that several clusters are close to each other, which will deteriorate the performance. Our method aims to project samples of each class into a subspace, thus samples can be well separated.

6. Conclusion

In this paper, we have presented a novel representation learning network, which is guided by sample relations learned by the network itself. To the best of our knowledge, it is the first effort to preserve both local neighborhood and global subspace consistency. Extensive experimental results on both small scale and large scale datasets have shown the superiority of the proposed method on similarity and representation learning over state-of-the-arts, including the latest deep learning based method. Note that our model is simple and fundamental, more complicated components, such as adversarial learning, label supervision, can be added to our framework to further improve the performance.

7. Acknowledgement

This paper was in part supported by Grants from the Natural Science Foundation of China (No. 61806045), the National Key R&D Program of China (No. 2018YFC0807500), the Fundamental Research Fund for the Central Universities under Project ZYGX2019Z015, the Sichuan Science and Technology Program (Nos. 2020YFS0057, 2019YFG0202), the Ministry of Science and Technology of Sichuan Province Program (Nos. 2018GZDZX0048, 20ZDYF0343, 2018GZDZX0014, 2018GZDZX0034).

8. References

References

- [1] A. Coates, A. Ng, H. Lee, An analysis of single-layer networks in unsupervised feature learning, in: Proceedings of the fourteenth international conference on artificial intelligence and statistics, 2011, pp. 215–223.
- [2] C. Tang, X. Zhu, J. Chen, P. Wang, X. Liu, J. Tian, Robust graph regularized unsupervised feature selection, *Expert Systems with Applications* 96 (2018) 64–76.
- [3] N. Dalal, B. Triggs, Histograms of oriented gradients for human detection, in: CVPR, 2005.

- [4] P. Vincent, H. Larochelle, I. Lajoie, Y. Bengio, P.-A. Manzagol, Stacked denoising autoencoders: Learning useful representations in a deep network with a local denoising criterion, *Journal of machine learning research* 11 (Dec) (2010) 3371–3408.
- [5] C. Tang, X. Liu, M. Li, P. Wang, J. Chen, L. Wang, W. Li, Robust unsupervised feature selection via dual self-representation and manifold regularization, *Knowledge-Based Systems* 145 (2018) 109–120.
- [6] Z. Zhang, Y. Zhang, G. Liu, J. Tang, S. Yan, M. Wang, Joint label prediction based semi-supervised adaptive concept factorization for robust data representation, *IEEE Transactions on Knowledge and Data Engineering* 32 (5) (2019) 952–970.
- [7] S. Huang, Z. Kang, Z. Xu, Auto-weighted multi-view clustering via deep matrix decomposition, *Pattern Recognition* 97 (2020) 107015.
- [8] X. Zhu, X. Li, S. Zhang, C. Ju, X. Wu, Robust joint graph sparse coding for unsupervised spectral feature selection, *IEEE transactions on neural networks and learning systems* 28 (6) (2017) 1263–1275.
- [9] X. Shen, S. Pan, W. Liu, Y.-S. Ong, Q.-S. Sun, Discrete network embedding, in: *Proceedings of the 27th International Joint Conference on Artificial Intelligence*, 2018, pp. 3549–3555.
- [10] Y. Bengio, P. Lamblin, D. Popovici, H. Larochelle, Greedy layer-wise training of deep networks, in: *Advances in neural information processing systems*, 2007, pp. 153–160.
- [11] M. Caron, P. Bojanowski, A. Joulin, M. Douze, Deep clustering for unsupervised learning of visual features, in: *Proceedings of the European Conference on Computer Vision (ECCV)*, 2018, pp. 132–149.
- [12] Z. Jiang, Y. Zheng, H. Tan, B. Tang, H. Zhou, Variational deep embedding: an unsupervised and generative approach to clustering, in: *Proceedings of the 26th International Joint Conference on Artificial Intelligence*, 2017, pp. 1965–1972.
- [13] K. Ghasedi Dizaji, A. Herandi, C. Deng, W. Cai, H. Huang, Deep clustering via joint convolutional autoencoder embedding and relative entropy minimization, in: *Proceedings of the IEEE international conference on computer vision*, 2017, pp. 5736–5745.

- [14] M. Jabi, M. Pedersoli, A. Mitiche, I. B. Ayed, Deep clustering: On the link between discriminative models and k-means, *IEEE Transactions on Pattern Analysis and Machine Intelligence* (2019) doi: 10.1109/TPAMI.2019.2962683.
- [15] X. QIAN, L. YAO, Extended incremental fuzzy clustering algorithm for sparse high-dimensional big data, *Computer Engineering* 45 (6) (2019) 75.
- [16] Y. Bengio, A. Courville, P. Vincent, Representation learning: A review and new perspectives, *IEEE transactions on pattern analysis and machine intelligence* 35 (8) (2013) 1798–1828.
- [17] J. Xie, R. Girshick, A. Farhadi, Unsupervised deep embedding for clustering analysis, in: *International conference on machine learning*, 2016, pp. 478–487.
- [18] X. Guo, L. Gao, X. Liu, J. Yin, Improved deep embedded clustering with local structure preservation., in: *IJCAI*, 2017, pp. 1753–1759.
- [19] B. Yang, X. Fu, N. D. Sidiropoulos, M. Hong, Towards k-means-friendly spaces: Simultaneous deep learning and clustering, in: *Proceedings of the 34th International Conference on Machine Learning-Volume 70*, JMLR. org, 2017, pp. 3861–3870.
- [20] X. Zhu, Y. Zhu, W. Zheng, Spectral rotation for deep one-step clustering, *Pattern Recognition* (2019) 10.1016/j.patcog.2019.107175.
- [21] J. Chang, L. Wang, G. Meng, S. Xiang, C. Pan, Deep adaptive image clustering, in: *Proceedings of the IEEE international conference on computer vision*, 2017, pp. 5879–5887.
- [22] P. Ji, T. Zhang, H. Li, M. Salzmann, I. Reid, Deep subspace clustering networks, in: *Advances in Neural Information Processing Systems*, 2017, pp. 24–33.
- [23] X. Chen, Y. Duan, R. Houthoofd, J. Schulman, I. Sutskever, P. Abbeel, Infogan: Interpretable representation learning by information maximizing generative adversarial nets, in: *Advances in neural information processing systems*, 2016, pp. 2172–2180.

- [24] P. Zhou, Y. Hou, J. Feng, Deep adversarial subspace clustering, in: Proceedings of the IEEE Conference on Computer Vision and Pattern Recognition, 2018, pp. 1596–1604.
- [25] N. Mrabah, M. Bouguessa, R. Ksantini, Adversarial deep embedded clustering: on a better trade-off between feature randomness and feature drift, arXiv preprint arXiv:1909.11832.
- [26] M. Yin, W. Huang, J. Gao, Shared generative latent representation learning for multi-view clustering., in: AAAI, 2020, pp. 6688–6695.
- [27] C. Zhang, Y. Liu, H. Fu, Ae2-nets: Autoencoder in autoencoder networks, in: Proceedings of the IEEE Conference on Computer Vision and Pattern Recognition, 2019, pp. 2577–2585.
- [28] X. Guo, E. Zhu, X. Liu, J. Yin, Affine equivariant autoencoder, in: Proceedings of the 28th International Joint Conference on Artificial Intelligence, AAAI Press, 2019, pp. 2413–2419.
- [29] S. Wang, Z. Ding, Y. Fu, Feature selection guided auto-encoder, in: Thirty-First AAAI Conference on Artificial Intelligence, 2017.
- [30] T. Hofmann, J. M. Buhmann, Pairwise data clustering by deterministic annealing, *Ieee transactions on pattern analysis and machine intelligence* 19 (1) (1997) 1–14.
- [31] C. Tang, J. Chen, X. Liu, M. Li, P. Wang, M. Wang, P. Lu, Consensus learning guided multi-view unsupervised feature selection, *Knowledge-Based Systems* 160 (2018) 49–60.
- [32] B. Scholkopf, A. J. Smola, *Learning with kernels: support vector machines, regularization, optimization, and beyond*, MIT press, 2001.
- [33] C. Tang, M. Bian, X. Liu, M. Li, H. Zhou, P. Wang, H. Yin, Unsupervised feature selection via latent representation learning and manifold regularization, *Neural Networks* 117 (2019) 163–178.
- [34] B. Schölkopf, A. Smola, K.-R. Müller, Nonlinear component analysis as a kernel eigenvalue problem, *Neural computation* 10 (5) (1998) 1299–1319.

- [35] C. Peng, Y. Chen, Z. Kang, C. Chen, Q. Cheng, Robust principal component analysis: A factorization-based approach with linear complexity, *Information Sciences* 513 (2020) 581–599.
- [36] J. B. Tenenbaum, V. De Silva, J. C. Langford, A global geometric framework for nonlinear dimensionality reduction, *science* 290 (5500) (2000) 2319–2323.
- [37] L. v. d. Maaten, G. Hinton, Visualizing data using t-sne, *Journal of machine learning research* 9 (Nov) (2008) 2579–2605.
- [38] Z. Zhang, Y. Sun, Y. Wang, Z. Zhang, H. Zhang, G. Liu, M. Wang, Twin-incoherent self-expressive locality-adaptive latent dictionary pair learning for classification, *IEEE Transactions on Neural Networks and Learning Systems*, doi:10.1109/TNNLS.2020.2979748.
- [39] R. Kannan, S. Vempala, A. Vetta, On clusterings: Good, bad and spectral, *Journal of the ACM (JACM)* 51 (3) (2004) 497–515.
- [40] C. Tang, X. Zhu, X. Liu, M. Li, P. Wang, C. Zhang, L. Wang, Learning a joint affinity graph for multiview subspace clustering, *IEEE Transactions on Multimedia* 21 (7) (2019) 1724–1736. doi:10.1109/TMM.2018.2889560.
- [41] J. Shi, J. Malik, Normalized cuts and image segmentation, *Departmental Papers (CIS)* (2000) 107.
- [42] K. Zhan, C. Zhang, J. Guan, J. Wang, Graph learning for multiview clustering, *IEEE transactions on cybernetics* 48 (10) (2017) 2887–2895.
- [43] Z. Ren, S. X. Yang, Q. Sun, T. Wang, Consensus affinity graph learning for multiple kernel clustering, *IEEE Transactions on Cybernetics*, doi:10.1109/TCYB.2020.3000947.
- [44] Z. Ren, Q. Sun, Simultaneous global and local graph structure preserving for multiple kernel clustering, *IEEE Transactions on Neural Networks and Learning Systems*, doi:10.1109/TNNLS.2020.2991366.
- [45] Z. Kang, X. Zhao, Shi, C. Peng, H. Zhu, J. T. Zhou, X. Peng, W. Chen, Z. Xu, Partition level multiview subspace clustering, *Neural Networks* 122 (2020) 279–288.

- [46] A. Y. Ng, M. I. Jordan, Y. Weiss, On spectral clustering: Analysis and an algorithm, in: Advances in neural information processing systems, 2002, pp. 849–856.
- [47] Z. Kang, H. Pan, S. C. Hoi, Z. Xu, Robust graph learning from noisy data, IEEE Transactions on Cybernetics 50 (5) (2020) 1833–1843.
- [48] C. Zhang, H. Fu, Q. Hu, X. Cao, Y. Xie, D. Tao, D. Xu, Generalized latent multi-view subspace clustering, IEEE transactions on pattern analysis and machine intelligence 42 (1) (2018) 86–99.
- [49] Z. Kang, X. Lu, Y. Lu, c. Peng, W. Chen, Z. Xu, Structure learning with similarity preserving, Neural Networks 129 (2020) 138–148.
- [50] W. Wang, Y. Huang, Y. Wang, L. Wang, Generalized autoencoder: A neural network framework for dimensionality reduction, in: Proceedings of the IEEE conference on computer vision and pattern recognition workshops, 2014, pp. 490–497.
- [51] G. Shakhnarovich, Learning task-specific similarity, Ph.D. thesis, Massachusetts Institute of Technology (2005).
- [52] D. Chen, J. Lv, Y. Zhang, Unsupervised multi-manifold clustering by learning deep representation, in: Workshops at the Thirty-First AAAI Conference on Artificial Intelligence, 2017.
- [53] P. Huang, Y. Huang, W. Wang, L. Wang, Deep embedding network for clustering, in: 2014 22nd International Conference on Pattern Recognition, IEEE, 2014, pp. 1532–1537.
- [54] M. M. Fard, T. Thonet, E. Gaussier, Deep k -means: Jointly clustering with k -means and learning representations, arXiv preprint arXiv:1806.10069.
- [55] M. Kheirandishfard, F. Zohrizadeh, F. Kamangar, Multi-level representation learning for deep subspace clustering, in: The IEEE Winter Conference on Applications of Computer Vision, 2020, pp. 2039–2048.
- [56] W. Huang, M. Yin, J. Li, S. Xie, Deep clustering via weighted k -subspace network, IEEE Signal Processing Letters 26 (11) (2019) 1628–1632.

- [57] C. Doersch, A. Gupta, A. A. Efros, Unsupervised visual representation learning by context prediction, in: Proceedings of the IEEE International Conference on Computer Vision, 2015, pp. 1422–1430.
- [58] D. Pathak, R. Girshick, P. Dollár, T. Darrell, B. Hariharan, Learning features by watching objects move, in: Proceedings of the IEEE Conference on Computer Vision and Pattern Recognition, 2017, pp. 2701–2710.
- [59] J. Wu, K. Long, F. Wang, C. Qian, C. Li, Z. Lin, H. Zha, Deep comprehensive correlation mining for image clustering, in: The IEEE International Conference on Computer Vision (ICCV), 2019.
- [60] J. Zhang, C.-G. Li, C. You, X. Qi, H. Zhang, J. Guo, Z. Lin, Self-supervised convolutional subspace clustering network, in: Proceedings of the International Conference on Computer Vision, 2019, pp. 5473–5482.
- [61] E. Elhamifar, R. Vidal, Sparse subspace clustering: Algorithm, theory, and applications, *IEEE transactions on pattern analysis and machine intelligence* 35 (11) (2013) 2765–2781.
- [62] G. Liu, Z. Lin, S. Yan, J. Sun, Y. Yu, Y. Ma, Robust recovery of subspace structures by low-rank representation, *IEEE transactions on pattern analysis and machine intelligence* 35 (1) (2012) 171–184.
- [63] Z. Kang, C. Peng, Q. Cheng, Kernel-driven similarity learning, *Neurocomputing* 267 (2017) 210–219.
- [64] D. P. Kingma, J. L. Ba, Adam: A method for stochastic optimization, in: Proc. 3rd Int. Conf. Learn. Representations, 2014.
- [65] P. Ji, M. Salzmann, H. Li, Efficient dense subspace clustering, in: Applications of Computer Vision (WACV), 2014 IEEE Winter Conference on, IEEE, 2014, pp. 461–468.
- [66] G. Liu, Z. Lin, S. Yan, J. Sun, Y. Yu, Y. Ma, Robust recovery of subspace structures by low-rank representation, *IEEE transactions on pattern analysis and machine intelligence* 35 (1) (2013) 171–184.
- [67] R. Vidal, P. Favaro, Low rank subspace clustering (lrsc), *Pattern Recognition Letters* 43 (2014) 47–61.

- [68] V. M. Patel, R. Vidal, Kernel sparse subspace clustering, in: Image Processing (ICIP), 2014 IEEE International Conference on, IEEE, 2014, pp. 2849–2853.
- [69] C. You, D. Robinson, R. Vidal, Scalable sparse subspace clustering by orthogonal matching pursuit, in: Proceedings of the IEEE conference on computer vision and pattern recognition, 2016, pp. 3918–3927.
- [70] X. Yang, C. Deng, F. Zheng, J. Yan, W. Liu, Deep spectral clustering using dual autoencoder network, in: Proceedings of the IEEE Conference on Computer Vision and Pattern Recognition, 2019, pp. 4066–4075.
- [71] X. Liu, M. Li, C. Tang, J. Xia, J. Xiong, L. Liu, M. Kloft, E. Zhu, Efficient and effective regularized incomplete multi-view clustering, *IEEE Transactions on Pattern Analysis and Machine Intelligence*, doi:10.1109/TPAMI.2020.2974828.
- [72] C. Peng, Z. Kang, S. Cai, Q. Cheng, Integrate and conquer: Double-sided two-dimensional k-means via integrating of projection and manifold construction, *ACM Transactions on Intelligent Systems and Technology (TIST)* 9 (5) (2018) 1–25.